

Design of an off-axis XR photovoltaic concentrator with SMS method

M. Zhang*, H. Dong, Z.J. Geng

State Key Laboratory of Management and Control for Complex Systems, Institute of Automation, Chinese Academy of Sciences, Beijing, China

ARTICLE INFO

Article history:

Received 18 October 2012

Accepted 19 March 2013

PACS:

42.79

Keywords:

Solar collectors and concentrators

Non-imaging optics

Photovoltaic

ABSTRACT

We present a novel off-axis XR concentrator design that enables a high efficiency energy collection while avoiding the shadowing problem encountered in the designs of symmetry XR type concentrator. Combining with a 1 cm² multi-junction solar cell, the off-axis XR concentrator is able to achieve high optical efficiency of the photovoltaic system. The concentrator design is performed based on the non-imaging optic principle, with one reflective mirror (X) and one refractive lens (R). Both surfaces of the reflective and refractive element are of freeform shapes and fitted as freeform expression in the design analysis. The concentrator has concentration ratio greater than 500× and acceptance angle greater than 2°. A square homogenizing irradiance distribution on the cell is achieved with the help of a suitable rob. The tolerance of the system is analyzed. The results show that the high concentration ratio and greater acceptance angle relax all optical and mechanical tolerances reduce the production and operation cost.

© 2013 Elsevier GmbH. All rights reserved.

1. Introduction

Photovoltaic technology is an effective method to harvest the solar resource. But the critical problems are to increase the solar-to-electrical conversion efficiency and reduce the cost.

Among existing solar photovoltaic (PV) technologies, concentrator cells have been reaching increasingly impressive efficiencies, inspiring new interest in the high-efficiency, high-concentration approach. Currently, multi-junction concentrator cells have achieved much higher efficiencies than that of any other approach, such as three-junction GaInP/GaInAs/Ge cell with the record efficiency of 40.7% [1,2]. However, Photovoltaic cells made of III-V materials are very expensive. One strategy for offsetting PV cell cost is to reduce the amount of semiconductor material needed, since the cost of silicon solar cells typically comprises more than one-half if the module cost.

The high concentration PV (CPV) technology is based on this strategy and it uses concentrating optics to focus the sun light onto small PV cell, thus uses smaller cell area to produce the same amount of electrical energy as large un-concentrated cell area.

The high concentration PV strategy is based upon several underlining assumptions:

- (a) *Direct radiation*: only direct radiation (not scattering sun light) contributes to high concentration PV modules, thus an active

tracking system is needed to keep the PV module facing the sun;

- (b) *High concentration rate*: the ratio N should be sufficiently high to make this scheme worthwhile. Typical ratio N is greater than 500 suns (one sun referring to maximum clear-sky solar normal beam radiation, about 1 mW/mm²);
- (c) *Glass/aluminum is cheaper than PV*: cost for optics and tracking components used for focusing the sun light should be cheaper than that of PV materials in the same size; and
- (d) *High Efficiency*: the efficiency of a high concentration PV module should be higher than that of a flat panel un-concentrated C-Si.

Optical design is the most critical technology that can ensure the validity of these assumptions [3]. Several typical optic systems have been put forward, including parabolic concentrator, compound parabolic concentrator, Fresnel lens and so on [4,5]. But these concentrators mentioned above have some disadvantage of low concentration ratio, small acceptance angle, difficulty to be fixed and serviced. Take Fresnel lens as example, once the sunlight moves 0.5 degree away from the straight direction, only 10% energy arrives at the cell.

Recently, several kinds of concentrators have been invented according to the non-imaging optics principle [6–15]. Comparing to imaging optics principle, which focus on the optical aberrations and image quality, non-imaging optics fundamentals pay more attention to transferring energy with high efficiency and making the light intensity uniform. Accordingly, it is successful to achieve such concentrator with uniform intensity, sufficient acceptance angle and high concentration. Some cases are presented here, as shown in Fig. 1.

* Corresponding author. Tel.: +86 10 62535832; fax: +86 10 62535832.

E-mail address: zhangmnk@gmail.com (M. Zhang).

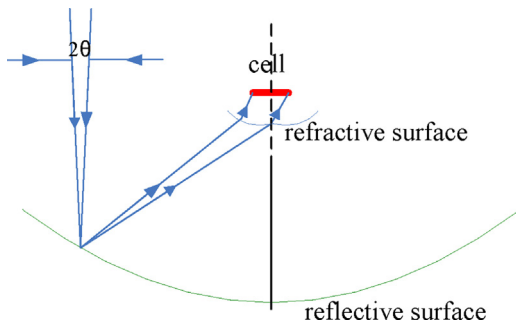


Fig. 1. XR Concentrators designed according to non-imaging optics.

Fig. 1 shows a kind of symmetric XR concentrator, which makes the light first reflect and then refract before reaching the receiver. Refractions are always denoted by R, reflections by X. The receiver is immersed in a medium of refractive index n . The concentration of this optic is higher than that of RR concentrator under the condition of equal acceptance angle. But the light transmission falls down, for the reason that the receiver faces in opposite direction as the concentrator's entry aperture. Meanwhile, the module assembling work of cell and radiator is too complex.

To solve the drawbacks mentioned above, an off-axis XR concentrator is proposed in this paper, which keeps the advantages of symmetric XR, while overcomes the receiver shadowing to promote the transmission, without wasting too much lens material. This kind of advanced concentrator could reduce costs for high concentration PV system for the reason of high optical efficiency, concentration ratio and high optical tolerance. In addition, advanced optical design technique can reduce the number of optical elements, and allow each optical surface to perform as many functions as possible.

The higher concentration the system has, the lower acceptance angle we can reach, and the higher reliability and accuracy the tracking system is remanded. Considering the manufacturing tolerance and overall cost, we design an off-axis XR concentrator with concentration ratio greater than $500\times$ and acceptance angle greater than 2° .

2. Design of the CPV

According to the non-imaging optic principle, the off-axis XR concentrator is designed by used of the hypothesis of edge rays principle and SMS 3D (Simultaneous Multiple Surface 3-dimension) method [6,7,16,17]. It is known that in the edge rays principle every edge ray passing through the borders of the entry aperture would definitely go out from the borders of the exit aperture. In SMS 3D design method the optical prescription is stated as incoming and outgoing wavefronts. The position of light source is regarded as infinite or finite distance with specific conditions. The concentrator is required to have a high concentration with $500\times$, acceptance angle not less than 2° and uniform illumination on the cell, when the high efficiency multi-junction cells are used in the system. This level of concentrator allows tolerances in mass production of all components, achieves high energy efficiency and decreases the costs of the structural elements.

The detailed design procedure is going to be described in this part, including four stages, as shown in **Fig. 2**:

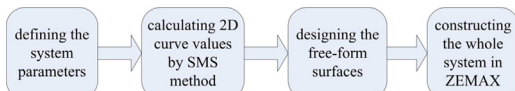


Fig. 2. The flow chart of the concentrator design.

- (a) Define the system parameters
- (b) Calculate 2D curve values of the reflector and refractor to obtain SMS initial discrete data
- (c) Design the two free-form surfaces according to the results of the step 2
- (d) Construct the whole system in ZEMAX optical soft

2.1. Defining the system parameters

Firstly, we can select the inputting parameters to calculate the concentrator as follows:

the size of the entry, the size of the receiver, the secondary lens refraction index n which is chosen as the medium of PMMA, the acceptance angle, the inclination angle of the receiver with respect to the x - y plane, an initial point P_0 on the mirror and the normal vector N_0 to the mirror at P_0 .

2.2. Calculating 2D curve values of the system by SMS method

Similar with SMS design for rotational XR concentrator, we first need to find a list of SMS points from reflector and refractor of the new XR optic with regard to the y - z plane. The details of the ray tracing in 2D is displayed in **Fig. 3**.

The input wavefronts, specified as planar ω_1 and ω_2 , simulate the sun radiation. The wavefronts are rotated by a small angle of θ to the left and right from the optical axis respectively, given the acceptance angle as θ . According to ray edge principle, the bundle of rays from ω_1 (such as the rays of r_1, r_3, r_5, \dots) should focus at the edge point R_2 on the receiver, while the rays from ω_2 (such as the rays of r_2, r_4, r_6, \dots) should focus at point R_1 .

As SMS design method described in some reference, we start from the edge point P_0 to obtain a subset of oval X_0X_1 on refractive surface. The edge rays r_1 and r_2 are defined to be particular to wavefront ω_1 and ω_2 , respectively. The rays with directions between those of r_1 and r_2 reflect at point P_0 . Then the Cartesian oval X_0X_1 on refractive lens concentrates the bundle on point R_1 , which means that the ray r_1 refracts at X_0 and the ray r_2 refracts at X_1 . The optical path length of rays r_1 and r_2 between points P_0 and R_1 should be equal by optic law. Since the normal vector at P_0 and the position of R_1 are all known, the points of oval X_0X_1 (and normal vector of every point) can be calculated by optic principle.

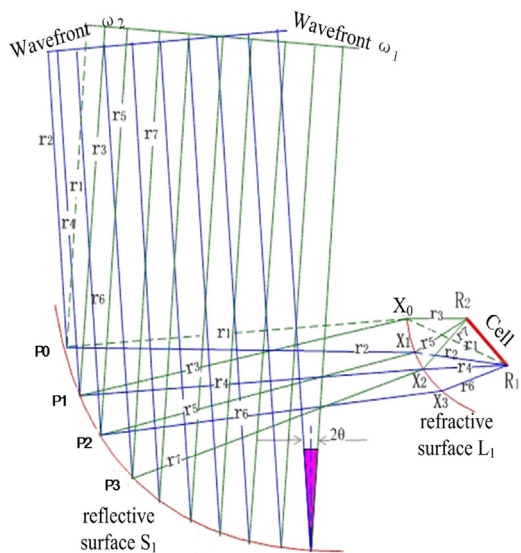


Fig. 3. The SMS 2D design procedure of the off-axis XR concentrator.

Then we can calculate the subset oval POP1 on reflective surface based on the point X0 already calculated. Similarly, we can launch a bundle of rays emitted from the receiver to refract at X0. These rays are contained between r1 and r3. Then we can obtain the Cartesian oval POP1 that makes them perpendicular to wave front ω_1 . Interpolate a low-order curve between P0 and P1 compatible with X0 and X1 to make it as smooth as possible.

Next we use portions POP1 and X0X1 to calculate the whole SMS 2D chains. A bundle of rays from ω_2 between r2 and r4 just impinge on the portion POP1 and finally focus at point R1. The ray r4 reflects from P1 toward X2. Deflections required along the path of r4 give us the position of X2 with its normal vector, as we know the optical path length of each ray from ω_2 to R1 is equal. Therefore the oval X1X2 can be constructed. Similarly, we can also launch a set of rays from R2 through the portion X0X1 of the refractive surface already calculated by inverting the Snell law. As shown in Fig. 3, the rays r3 and r5 from R2 reflect at portion P1P2 and finally impinge on wavefront ω_2 , with equal optical path length. After that, the oval P1P2 is calculated. The calculation of points can be repeated to get a sequence of points with normal vectors of both surfaces in the $x=0$ plane. We can call the sequence of points on reflective surface as S1 while L1 on refractive surface. Choose a new initial input value to calculate, if illogical curve of some shadow occurs.

2.3. Defining the two free-form surfaces of the concentrator

The SMS chain L1 and S1 obtained from last step is taken as inputting data in this step. In this part the whole surface of the reflective mirror and refractive lens is going to be constructed, applying 3D SMS method. As shown in Fig. 4(a), two planar wavefronts ω_3 and ω_4 are rotated by a small angle of θ to the left and right with respect to plane $x=0$ respectively. The rays emitted from ω_3 and ω_4 finally focus at the edge points R3 and R4 respectively. Fig. 4(b) gives the position of R1, R2, R3 and R4 on the receiver. We can start with the rays from ω_3 . The edge ray from ω_3 reflects at P0 and then refracts at a new point of the lens. The ray tracing procedure is just similar with that mentioned in step 2. We repeat the ray tracing calculation for all the points at chain L1 between ω_3 and

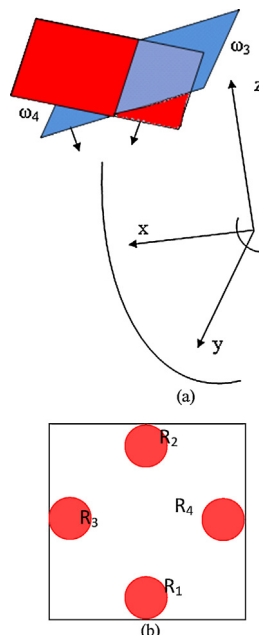


Fig. 4. (a) Two planar wavefronts ω_3 and ω_4 rotated by a small angle of θ to the left and right with respect to plane $x=0$. (b) The position of R_1 , R_2 , R_3 and R_4 on the receiver.

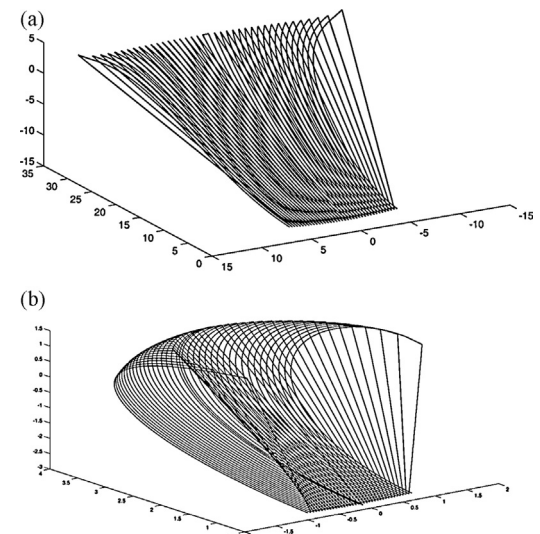


Fig. 5. (a) SMS 3D data of reflective surface in matlab software. (b) SMS 3D data of refractive surface in matlab software.

R4. After that, a new chain on the lens near S1 is achieved. Make the new chain as inputting data and trace the ray from R3 toward ω_4 . Then a new chain on the mirror is achieved. Before finishing enough data calculation, we repeat the procedure.

All the procedure is finished by use of Matlab software. The SMS 3D data of reflective surface and refractive surface is shown in Fig. 5.

Finally, we fit all data of the two surfaces to free-form curves which must be consistent with that in ZEMAX optical software. The mirror and lens profile can be described as the form below:

$$z = \frac{cr^2}{1 + \sqrt{1 - (1+k)c^2r^2}} + \sum_{i=1}^N A_i E_i(x, y) \quad (1)$$

where z is coordinate data of the surface, c is the base curvature at the vertex, k is a conic constant, r is the radial coordinate measured perpendicularly from the optical axis, A_i is the coefficient of the high-order polynomial, and $E_i(x, y)$ is the polynomial function with x and y .

2.4. Constructing the whole system in ZEMAX

The two surfaces are introduced into ZEMAX software. The source property can be defined in software accordingly. The material of lens is set as PMMA. The structure of the concentrator is finished and illuminated in Fig. 6(a). The size of incident aperture is about 21 cm \times 26 cm, which means that the concentration of the system is about 546.

There is a transparent rod adhered or molded together with the refractive lens, which is just a well known homogenizing device in Non-imaging optics. The cell is just adhered to the other end of the rod, which can make a great deal to reduce the peak concentration for a homogenized irradiation on the cell. The incident size of rod is about 11.2 mm, which is defined as the size of receiver for the initial inputting parameter. The exit aperture of the rod is equal to the size of cell with 10 mm. So there is a little gradient for its four side faces, which is helpful to get total internal reflection for most of the incident rays. The rod also can be mirror-coated so that wider-angle rays that miss the cell are finally reflected onto the cell. The longer is the length of rod, the better homogenization we can get. But the rod used here is not more than 20 mm because the illumination angle of the cell in the concentrator

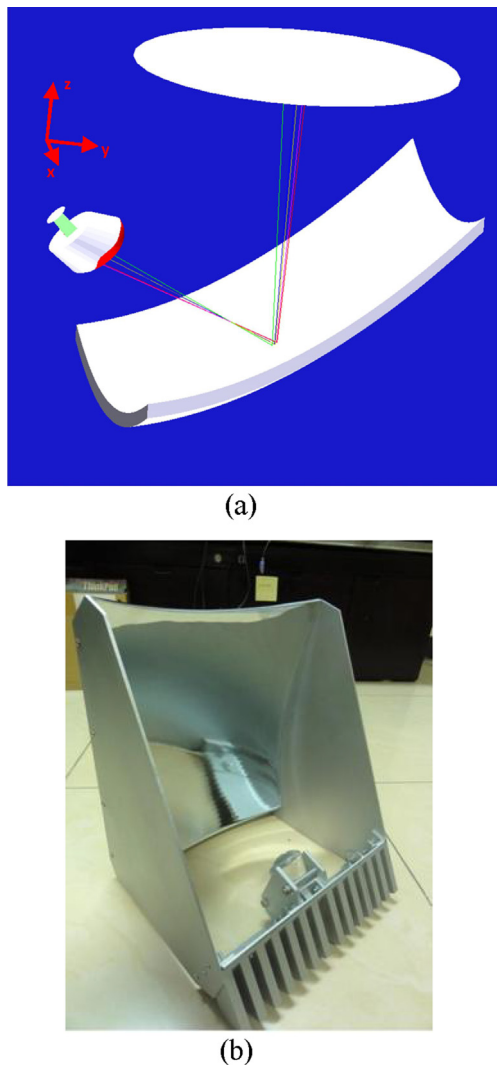


Fig. 6. (a) The construction of the concentrator. (b) View of a fixed concentrator sample.

is very wide. A real concentrator sample is fixed and shown in Fig. 6(b).

3. Analysis of the CPV system

3.1. Performance analyses of the off-axis XR concentrator

Analyses about the off-axis XR concentrator is presented in this section, including optical efficiency, irradiance distribution on the concentrator exit aperture and the angular transmission. Additionally, the optic tolerance analyses of the system are presented later, such as the effect of the misalignment of the system on the optical efficiency.

The optical efficiency and the acceptance angle, as two important critical parameters, are represented from the angular transmission curve. The optical efficiency of the concentrator is generally defined as the maximum transmission which is occurred when the incident angle is zero. Actually, some energy may loss, because the cell coating may reflect part of the radiation. But the definition here is always described as ratio of the power on the exit aperture of rod over the power of a parallel beam reaching the entry aperture.

The acceptance angle is defined as the angle which is happened when the optical efficiency just falls down to a 90% of the maximum.

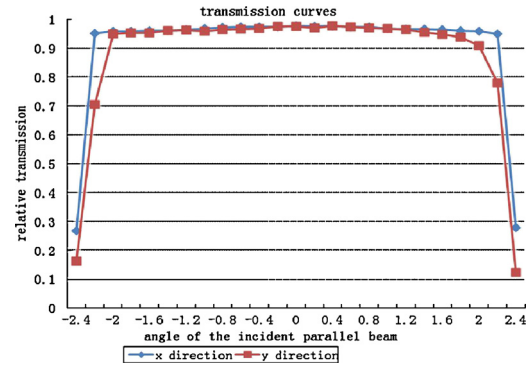


Fig. 7. The relationship between optical efficiency and the field-of-view.

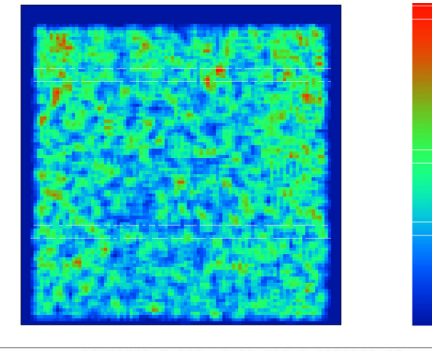


Fig. 8. The irradiance distribution on the solar cell. (For interpretation of the references to color in the text, the reader is referred to the web version of the article.)

The direction of the incident parallel beam can be determined with two directions, from positive to negative of x and y respectively. The figure gives the transmission curves for both sections. As Fig. 7 shown, the optical efficiency is about 98.2% without regard to the loss of the mirror reflectivity. For x section, the optical efficiency is not lower than 95.49% over the range of $\pm 2.2^\circ$, while for y section it is not lower than 90.9% over the range of $\pm 2^\circ$.

Fig. 8 shows the irradiance distribution on the solar cell under the condition of the straight sunlight incident. In this figure, the intensity of the irradiance is increased as the color from blue to red. It can be seen that the color does not change too much, which means that the intensity is nearly uniform. And the shape of the spot is also square matching with the size of the cell.

3.2. Tolerance analyses of the off-axis XR concentrator

It is very important for CPV system to have high tolerance, because it helps directly to know influences of misalignment on the performance of the whole system. A good optical system with high tolerance could lower cost for fabrication of optics, module assembly, system integration and maintenance, and finally reduce overall system cost significantly. In this section we provide the tolerance analyses of the CPV system in case of displacement and twist of different part of the concentrator.

Table 1

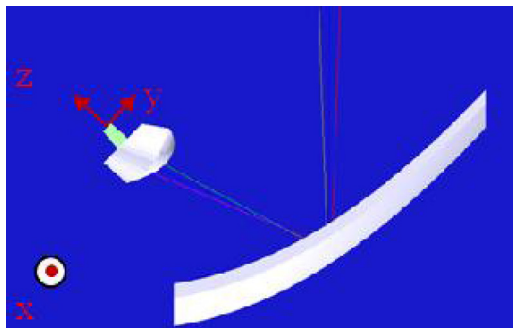
Tolerance about the relative displacement of the cell.

	Nominal value	Displacement	
		x direction (2 mm)	y direction (2 mm)
Transmission	97.78%	75.89%	78.74%
x section	2.2	2.2	2.2
y section	2.1	2.1	2.1

Table 2

Tolerance about the relative displacement and twist of the lens + cell.

	Nominal value	Displacement			Twist		
		x direction (2 mm)	y direction (2 mm)	z direction (2 mm)	x (2°)	y (2°)	z (2°)
Transmission	97.78%	97.42%	96.55%	97.12%	94.26%	97.51%	97.55%
x section	2.2	1.6	2.3	2.2	1.7	1.2	2.1
y section	2.1	2	1.7	1.7	1	2	2

**Fig. 9.** The direction of variation of relative position for the cell in z-y plane.

Two types of variations have been considered, which are positioning error of cell respect to the rest of the system, and positioning error of union of refractive lens and cell respect to the primary reflective mirror. Then the variables of optical efficiency and acceptance angle are analyzed. The analyses of the cell relative displacement are indicated in **Table 1**, while the varying directions of the cell (x, y, z) are shown in **Fig. 9**.

The result for displacement and twist of the lens + cell is indicated in **Table 2**, while the varying direction is similar as the coordinate axis in **Fig. 7**. We can see that there are not significant changes of transmission with relative variation between the lens + cell and the mirror. But when moving only a cell, the optical efficiency is decreased to 78.74% for the y direction. The main reason is the loss of the receiving area on the cell.

4. Conclusions

An off-axis XR concentrator for high efficiency multi-junction solar cells has been presented in this paper. It has been designed based on the non-imaging optic principle, which is expressed by the simultaneous surface design method and edge ray principle. The reflective mirror and the refractive lens are all fitted as free-form surfaces. The concentrator has high concentration no less than 500× and acceptance angle no less than 2°, which relax all optical and mechanical requirements. The characters of concentrator, such

as high optical efficiency, high concentration ratio and tolerance, contribute to reduce overall system cost significantly. The sample of the concentrator has been processed and tested.

Acknowledgements

This work has been supported by the National High-tech R&D Program (863 Program) of CASIA (Chinese Academy of Sciences, Institute of Automation), Grant No. 2012AA011903.

References

- [1] S.Kurtz, Opportunities for development of a mature concentrating photovoltaic power industry, in: CS MANTECH Conference, May 18–21, Tampa, FL, USA, 2009.
- [2] L.M. Fraas, Toward 40% and higher solar cells in a new cassegrainian PV module, in: Photovoltaic Specialists Conference, 31st IEEE, IEEE Piscataway, Lake Buena, FL, 2005.
- [3] V. Gurboushian, R. Gordon, Optical design considerations for high-concentration photovoltaics, in: Proc. SPIE, vol. 6339, 633905/1-9, 2006.
- [4] J.S. Lin, W.C. Huang, H.C. Hsu, et al., A study for the special Fresnel lens for high efficiency solar concentrators, in: Proc. SPIE, vol. 5942, 59420X/1-9, 2005.
- [5] P. Gleckman, A high concentration rooftop photovoltaic system, in: Proc. SPIE, vol. 6649, 664903X/1-10, 2007.
- [6] P.A. Davies, Edge-ray principle of nonimaging optics, *J. Opt. Soc. Am. A* 11 (1994) 1256–1259.
- [7] R. Winston, J.C. Miñano, P. Benítez, Nonimaging Optics, Elsevier Academic Press, San Diego, 2004.
- [8] J.C. Miñano, J.C. Gonzalez, P. Benítez, A high-gain, compact, nonimaging concentrator: RXI, *Appl. Opt.* 34 (1995) 7850–7856.
- [9] J.C. Miñano, J.C. Gonzalez, P. Benítez, New non-imaging designs: the RX and the RXI concentrators, in: Proc. SPIE, vol. 2016, 1993, pp. 120–127.
- [10] M. Hernández, P. Benítez, J.C. Miñano, et al., The XR nonimaging photovoltaic concentrator, in: Proc. SPIE, vol. 6670, 667005, 2007, pp. 1–10.
- [11] J.C. Miñano, P.P. Gonzalez, Design of nonimaging lenses and lens-mirror combinations, in: Proc. SPIE, vol. 1528, 1991, pp. 104–115.
- [12] W.A. Parkyn, F. Munoz, J.C. Miñano, et al., Edge-ray design of compact etendue-limited folded-optic collimators, in: Proc. SPIE, vol. 5185, 2004, pp. 6–17.
- [13] J.L. Alvarez, M. Hernandez, P. Benítez, et al., TIR-R concentrator: a new compact high-gain SMS design, in: Proc. SPIE, vol. 4446, 2002, pp. 32–42.
- [14] A. Bielawny, P.T. Miclea, A.V. Rhein, et al., Dispersive elements for spectrum splitting in solar cell application, in: Proc. SPIE, vol. 6197, 619704, 2006, pp. 1–8.
- [15] S. Kudaev, P. Schreiber, Optimization of symmetrical free-shape non-imaging concentrators for LED light source applications, in: Proc. SPIE, vol. 5942, 594209, 2005, p. 1210.
- [16] P. Benítez, et al., Simultaneous multiple surface optical design method in three dimensions, *J. Opt. Eng.* 43 (2004) 1489–1502.
- [17] J. Chaves, Introduction to Nonimaging Optics, CRC Press, New York, 2008.